MJSAT

Malaysian Journal of Science and Advanced Technology

journal homepage: https://mjsat.com.my/

Recent Advances in SILAR-deposited Metal Sulfide Films

Ho Soonmin*

[1]*Faculty of Health and Life Sciences, INTI International University, Putra Nilai, 71800, Negeri Sembilan, Malaysia.*

KEYWORDS

Thin films
Metal chalcogenide
Band gap
Solar cell applications

ARTICLE HISTORY

Received 4 August 2025
Received in revised form 25 October 2025
Accepted 17 November 2025
Available online 7 December 2025

ABSTRACT

Many researchers have reported physical, and chemical deposited thin films. Nevertheless, the deposition methods had a strong effect on the properties of the produced films. SILAR method has been used to produce different thin films for various studies over the years. Alternative deposition methods have attracted extensive attention while this approach has several advantages. Seemingly, high area deposition could succeed at low temperatures, with standard inexpensive equipment, without the requirement of a vacuum chamber and some unique films properties could be controlled. The SILAR process usually includes four stages; adsorption, a wash, reaction and second wash were performed to rinse off unreacted species. SILAR method was used to deposit a thin film of metal sulfides on substrates in this study. The primary outcomes are the characterization of the films and their application after finishing. It was observed that the number of deposition cycles, rinsing time, immersion duration and precursor concentration affected the crystallinity, grain size, film thicknesses and surface morphologies of the deposited films. Furthermore, the results confirmed these films for solar cells, sensors and supercapacitors applications. The power conversion efficiency also improved of Cu_2SnS_3 about 0.11% and copper zinc tin sulfide were found to be 0.396%, respectively.

1. INTRODUCTION

Thin films have garnered significant attention due to their exceptionally unique properties. Several deposition methods have been reported to synthesize thin films successfully [1]. The deposition techniques encompass electrodeposition, chemical bath deposition [2], chemical vapor deposition, flash evaporation, thermal evaporation [3], vacuum evaporation, pulsed laser deposition [4], sol-gel technique, atomic layer epitaxy [5], sputtering, successive ionic layer adsorption and reaction (SILAR) and spin coating method. The prepared films may serve in lasers [6], cathode ray tubes, optoelectronic applications, solar cells [7], laser and sensor devices.

N-type semiconductors are formed by introducing impurities with a higher number of valence electrons than the semiconductor material such as silicon or germanium into them. Common dopants for n-type semiconductors are phosphorus and arsenic.

The additional electrons provided by the dopant become free electrons, serving as the majority charge carriers in n-type semiconductors. N-type semiconductors have a large density of negative charge carriers which enables them to effectively conduct negative charges. [8] P-type semiconductors displayed a significant abundance of positive charge carriers (holes) which allow them to effectively conduct positive charges. P-type semiconductors are formed by introducing impurities with fewer valence electrons than the semiconductor material being doped [9]. Typical dopants for p-type semiconductors are boron and gallium. The absent electron served as positive charge carriers in p-type semiconductors, enabling the flow of positive charges.

The benefits of the SILAR method consist of extensive area deposition that can be performed on any substrate at lower temperatures through straightforward technique and cost-effective tools [10]. It allows for control over stoichiometry, film thickness, morphology, and grain size. Also, this method conserves materials and reduces production costs, eliminates

*Corresponding author:
E-mail address: Ho Soonmin < soonmin.ho@newinti.edu.my >.
https://doi.org/10.56532/mjsat.v5i4.586

the need for vacuum chamber, provides an impressive growth rate and prevents the formation of precipitates in the container [11]. Typically, SILAR involves four stages: adsorption where cations adhere to the substrate surface, an initial rinse with water to wash away excess adsorbed ions, the reaction phase where anionic ions are introduced into the system, and a second rinse to remove any unreacted species and surplus ions.

Tellurium is not metal but instead a metalloid or semimetal showing some properties of both metals and nonmetals. It is a brittle, silvery-white, weak-key alkaline metal which may be PH 12–13 in the grade somewhat found as crystals. Tellurium is one of the less common elements; it has the same rarity as platinum. Even at very low doses, tellurium can be toxic to animals and humans. Continuous tellurium exposure also threatens the kidney, liver and the nervous system. However, the exposure of Tellurium may lead to headache, fatigue, dizziness and somnolence or weakness. Side-effects of garlic include the breath smelling of garlic and it may cause nausea if overconsumed repeatedly.

Selenium is a nonmetal, not as meander that has the synthetic image Se and nuclear number 34. It occurs naturally in many forms, including a gray metallic looking allotrope which is most common under normal conditions. Selenium is a vital nutrient in limited quantities, but it can lead to toxicity if consumed beyond the level. Toxicity: excessively high levels of selenium in the body can cause toxicity, with symptoms that include hair loss, fatigue, and occasionally vomiting; severe cases of selenium toxicity may lead to an organ failure.

Metal sulfides have been explored on account of their fascinating properties and display promise for potential applications in diverse fields. Because of their interesting optoelectronic properties, poor to very low solubility, and tunable behavior they are highly desirable for research in solar energy storage, water splitting, solar cell application and wastewater treatment areas.

Metal sulfides are, of course, common earth minerals. They are produced by the combination of sulfur with other metals and semi-metals in varied ratios. These two compounds are valuable in different places. Materials such as metal sulfides show good electrical conductivity, low redox potential and chemical stability. The sulfur:metal ratio may take different values leading to different compounds, such as MS, M2S, M3S4 and MS2 (M represents metal).

Metal sulfides are a type of compound formed by the combination of sulfur with one or more metal elements [12]. Nanomaterials made of metal sulfides are promising options for various applications in medicine, biology, environmental science and energy generation, owing to their ability to absorb light, excellent optical properties, high specific capacitance and photocatalytic abilities. Sulfur is typically regarded as safer than tellurium because of its lower toxicity and its role as an essential element for life, whereas tellurium is viewed as a non-essential element that may have toxicological effects. Conversely, sulfur is mostly regarded as non-toxic, while selenium is a crucial trace element that may become toxic in excessive amounts, and selenium sulfide is likely a human carcinogen.

China produced roughly 19 million metric tons of sulfur in 2024, making it by far the world's largest sulfur producer (Table 1). Sulphur is also one of the abundant chemical elements in nature. It is a brittle solid with a pale-yellow hue, odorless, and has a bitter taste. The US is the second largest producer of Sulfur in the world, behind Saudi Arabia, and Russia. By 2024, the US sulfur production was reportedly approximately 8.2 million metric tons. Of that total, about 91 percent was recovered which was elemental sulfur.

In this study, the researcher will outline the preparation of films of metal sulfides, through SILAR deposition method. The mechanisms of thin film growth will be emphasized. The properties and uses of the acquired nanostructured thin films will be studied.

Table 1. Worldwide production of sulfur in 2024.

Country	Production (in 1000 metric tons)
China	19000
United States	8200
Saudi Arabia	7500
Russia	7500
United Arab Emirates	6000
Kazakhstan	5100
Canada	5000
India	3700
Japan	3100
South Korea	3100
Qatar	3100
Iran	2000

2. METHODOLOGY

To identify the research articles published between 1996 and 2025 in PubMed, Google Scholar, Taylor & Francis, ACS, Web of Science, Wiley Online Library, Scopus, Science Direct and MDPI, the authors performed a literature search in appropriate journals. The terms used included "thin films", "metal sulfide", "SILAR method", "sensor", "supercapacitor", "photovoltaic applications", "band gap", "deposition technique", and "semiconductor".

3. LITERATURE SURVEY

3.1 Cobalt tin sulphide

Preparation of CoSnS films on glass slides using ammonia, cobalt sulfate, thioacetamide and tin chloride [13] with time (rinsing time=10 s, immersion time=20 s). XRD studies confirmed that the existence of secondary phases including Sn2S3, CoS, Co9S8 and SnS2. Optical investigations revelated that absorption was extremely high at wavelengths under 350 nm. Refractive index decreased from 3.11 to 2.94, whereas the band gap increased from 1.22 eV to 1.52 eV, and electronegativity rose from 1.6928 to 1.7168, as the deposition cycles increased from 40 to 80.

The refractive index is a fundamental property of an optical material. The refractive index is also highly correlated with the electronic polarization of ions and the local field in the optical material. Naturally source plays a crucial role in selecting the material for opto-electronic devices like optical switches, modulation, filters and other electronic devices. It was noticed that the refractive indices of CoSnS semiconducting compounds exist between those of its binary components CoS

and SnS (3.5–5.5) and they are reasonably at par with the reported values.

Optical electronegativity is a key parameter characterizing many physical properties of optical material. The optical electronegativity of an atom and its power to attract electron in ionic crystal can be measured theoretically in model. The optical electronegativity gradually rose from 1.6923 at 40 cycles to 1.7168 at 80 cycles. The optical electronegativity of CoSnS thin films may have increased because the material was a refractive index-dependent material that decreased with deposition cycles. Furthermore, the low value of the estimated optical electronegativity and the high refractive index values of the material might also be attributed to the nature of the bond in the CoSnS system.

3.2 Bismuth sulfide

Bismuth sulfide (Bi_2S_3) films were synthesized using 2-methoxyethanol to manage the solubility of bismuth ions. Orthorhombic phase films were prepared, and the band gap was 1.6 eV. The peak photocurrent density attained was 1 mA/cm^2 in photoelectrochemical cells [14]. Better crystallinity [15] with higher absorption value (exceeding 10^4 cm^{-1}) could be seen in anneal films (200 °C).

The n-type films were deposited onto glass slide at room temperature [16]. The annealing process was conducted at 250 °C for 30 minutes in air. SEM studies showed grains entirely covered the substrate's surface. The improvement in photosensitivity was evident in annealed films, rendering these materials highly beneficial for sensor applications. The production of the films may be conducted with bismuth nitrate [17], TEA and sodium sulphide on stainless steel (70 deposition cycles). The strongest diffraction peak could be found in (111) plane, and crystallite size was 34 nm. SEM images verified the porous nanostructure, which could offer enhanced kinetics for electrochemical reactions. Energy density, specific capacitance and power density 8.89 Wh/kg at 1.4 Ag^{-1}, 289 F/g and 1147 W/kg at 3.2 Ag^{-1}, respectively.

Morphology studies were conducted and showed [18] that a clustered morphology, featuring small hillocks with a relatively uniform distribution based on AFM images. Optical studies indicated a direct band to band transition, with the assessed band gap diminishing from 181 eV to 1.25 eV as cationic concentration rises from 0.01 M to 0.03M. Electrical resistivity investigation showed a negative temperature coefficient of resistance, validating the semiconducting characteristics of Bi_2S_3 films. The activation energy decreased from 0.059 eV to 0.022 eV as the cationic concentration increased, a change attributed to enhanced grain size and diminished defect levels.

Formation of films at lower temperature using bismuth nitrate (cation) and thioacetamide (anion) [19]. XRD investigations indicate that the prepared films are amorphous, while they display a nanocrystalline structure following an annealing at 573 K. Optical analyses reveal that the absorption spectrum arises from transitions between bands and is predominantly driven by allowed direct transitions. The reduction in energy activation from 0.65 to 0.36 eV results from the quantum size effect.

3.3 Molybdenum sulphide

Molybdenum sulfide (MoS_2) exhibits distinct properties like adjustable band gap values and flexible mechanical characteristics. During the experiment, formation of thin film was conducted on different types of substrates [20]. Study results indicated that these films possess a suitable band gap (1.3 eV) and a remarkable absorption coefficient value ($2.8x10^6$ cm^{-1}). The resistivity as a function of temperature decreases with increasing of temperature, implying that the film is semiconducting. The resistivity at 27 °C was of the order of 10^4 Ωcm. The p-n junction nature of the film was confirmed from the thermos electric power study, the film being p-type in electrical conduction type.

Thin films were deposited on quartz [21] using sodium sulfide and sodium molybdate solutions. SEM images showed full coverage with MoS_2 flakes in the as-deposited films, suggesting that the orientation of the basal planes of MoS_2 could be perpendicular to the surface of the substrates. The annealed film clearly illustrates the merging of flakes into one another, creating stacked layers. The elemental ratio of sulfur to molybdenum in as-deposited and annealed sample measured by energy dispersive x-ray spectroscopy was observed to be close to 2, indicating the production of MoS_2. The elemental ratio of sulphur to molybdenum stayed the same even after annealing. A higher band gap (2eV) was noted in the as-deposited films in comparison to the annealed samples (1.72 eV). The detected change was likely a result of the enlargement in particle size brought about by the coalescence of MoS_2 flakes.

It has been observed that annealed semiconductor samples should have a lower band gap than as-deposited samples. This behaviour has a well-known effect on various semiconductor materials when annealed. With the increasing anneal time, the grains grow, and removals of the defects happen, leading to a variation in the electronic band structure, which causes a shift of band edges and thus a decrease of the band gap. This decrease in the band gap may be desirable for certain applications, such as in solar cells where a narrower band gap may allow for more absorption of visible and near infrared red (IR) light.

3.4 Lead sulphide

Soda lime glass and TEA were used as substrate and complexing during the formation of films [22]. Rough surface texture, and the most prominent diffraction peak associated with the (200) plane could be observed as shown in SEM and XRD studies. Cubic phase could be seen when the films have been prepared on silicon (100) and silicon (111) substrates [23]. On the other hand, crystalline size and thickness were found to be 480 nm and 18.6 nm using glass slides [24]. Cubic phase was observed, and the band gap was 1.77 eV. It was noticed that It was noted [25] that the immerse cycle affected the properties of films such as refractive index, extinction co-efficient, and imaginary dielectric constants. In XRD studies, the strongest diffraction peak has been transferred from (111) to (200) plane when the dipping cycle was increased. The impact of pH on film characteristics has been documented [26]. Based on XRD data, crystallite sizes (16-23 nm), and an enhancement in crystallinity was noted with rising pH values. Room temperature resistivity ($1.2x10^7$ to $3.5x10^7$ Ωcm) were also determined.

Nanostructured PbS could be used in gas sensor applications as described [27]. Stoichiometric compounds could be supported through XPS results. FESEM exhibited distinctly visible dense grains when the concentration of

precursor was 0.25M. Thickness and grain size were measured at 232.9 nm and 100 nm, respectively. Additionally, they clarified that these films showed the greatest sensitivity due to having the roughest surface, which significantly increased the net surface area, resulting in a higher total number of sites available for gas adsorption.

In various sensing applications, an increased surface roughness may provide more sensitive detection because of a larger surface area and the localized surface plasmon effect that may enhance binding or reaction to target species. On the other hand, roughness can reduce sensitivity, for instance in fiber optic sensors, where it perturbs light propagation. In the end, the role of roughness on sensitivity will be application and process dependent on whether the surface roughness directly affects the sensing mechanism. Irregular surfaces are known to offer higher surface areas for the interacting of the target analyte, thereby generating a stronger signal and sensibility. Furthermore, the roughness can increase the localized surface plasmon resonance, which is important for some optical sensors, and thus maximize the sensitivity.

A commonly used semi-conductor material in sensor applications is lead sulfide, possessing a tunable bandgap for high optical absorption and good processing. Specifically, the film is ideal for gas sensors and photodetectors, such as those used in infrared and X-ray detection. This material, upon gas exposure, is used to form resistance in gas sensors and can be detected for various gases such as NH_3, NO_2, SO_2, H_2S, and CH_4. PbS quantum dots (QDs) with intelligent features of versatile bandgap and dominant absorption availability an important material for both visible & near infrared photodetectors. Given their high atomic number and tunable bandgap, PbS QDs are considered as a promising interferer for X-ray detection. PbS has a tunable bandgap that allows it to be used for mid infrared (IR) and far IR LEDs and photo detectors.

Although both sputtering and SILAR methods have developed thin films for sensors, it was observed that the sputtering technique produces better properties such as adhesion, uniformity and purity in the films, which are highly recommended for some important sensor's applications. Nevertheless, SILAR method provides some advantages in relation to cost and simplicity of deposition, especially when dealing with certain substrate materials and at risk for high temperature processing.

3.5 $CuInS_2$

Several types of substrates could be employed for the formation of films. Soda lime glass [28] has been used as substrate in the presence of $InCl_3$, $CuSO_4$, and CH_4N_2S. The stoichiometric of $CuInS_2$ was prepared on glass substrate [29] through $InCl_3$, Na_2S, and $CuCl_2$ and showed the tetragonal phase [30]. In terms of photovoltaic properties, fill factor, efficiency was 0.31, and 0.92%, respectively. Annealed films (200 °C, 1.5 hours) were synthesized as proposed by Fanghong and co-workers [31]. Well crystallized samples exhibited rich in sulfur compositions. Zhengguo and co-workers [32] concluded that resistivity and stoichiometric were highly influenced by the [Cu]/[In] ratio.

$CuInS_2$ is a potential candidate for solar cell materials. It is known for its naturally advantageous optical properties, inexpensive price, non-toxicity and comparably merge synthesis. It is a potential absorber for thin-film solar cells, and its properties can be adjusted by particle size. The size of $CuInS_2$ nanoparticles is applicable to be varied, but the corresponding energy gap and absorption spectrum, to modulate in the entire visible and near infrared region.

3.6 Iron sulphide

Iron sulfide is a group of chemical compounds and minerals with the formula Fe_xS_y. The proportion of iron and sulfide of FeS films differ to each proportion. Depending on Fe/S concentration, the material will be present in various phases (pyrrhotite, troilite, mackinawite, greigite and pyrite). Thus, these materials possess distinct crystalline structures. Pyrites are currently gaining much interest due to the possibility of producing low cost.

The FeS deposited onto substrates using SILAR method at a concentration of 0.15 M (with TEA present) exhibited the optimal nanocrystal structure [33]. Basically, TEA is commonly used as a complexing agent in many of the chemical methods of thin film deposition. It functions as a chelate for metal ions controlling the release of ions during deposition and in turn affects film characteristics such as morphology, crystallinity and thickness. Typically processing methods that do not involve a vacuum will result in reduced production costs. The films generated might be utilized for solar cell applications because of their outstanding transmittance characteristics and high absorption coefficient (greater than $5x10^5$ cm^{-1}, wavelengths below 700 nm). Moreover, these films displayed p-type characteristics, possessing hole mobilities of approximately 100 cm^2/Vs. These results suggest that the values of micro strain and dislocation strain are decreased with enhancing the concentration of the FeS thin film. The crystallinity and the crystallite size have also been found to increase with the increase in the molar concentrations of the substrates.

3.7 MnS

As an important supercapacitor electrode material, MnS (Manganese Sulfide) stands out because of its high theoretical specific capacitance, good stability, and low price. Its super capacitive behavior is due to the charge storage occurring by both electric double layer capacitance and faradaic processes [34]. MnS may be accommodated with various crystal structures such as α-MnS (rock salt), β-MnS (Zinc-Blende), and γ-MnS, which would also affect the electrochemical behaviors of MnS. Pseudocapacitance is a phenomenon that stores electrical energy faradaically in electrochemical capacitors, performed by fast and reversible redox reactions or intercalations on the electrode surface. It fills the gap between the electrochemical double-layer capacitor and the rechargeable battery by providing a higher energy density than electrochemical double-layer capacitors, and a higher power density than batteries.

The uniform grain and polycrystalline phase could be observed as shown in XRD patterns and SEM images when the substrate was glass slide. Band gap (3.39 eV to 2.92 eV) and resistivity ($11.84x10^6$ to $2.21x10^5$ Ωcm) decreased as film thickness increased from 180 nm to 350 nm. Sodium sulfide and manganese acetate were used to produce films onto stainless steel [35].

Thin films are frequently formed on the surface of stainless steel because it is a nonreactive metal and resists corrosion. Several techniques, such as physical vapor deposition techniques including electron beam physical vapor deposition

and magnetron sputtering and chemical vapor deposition and the like, are employed to fabricate thin films on stainless substrates. These coatings can improve characteristics such as corrosion resistance, wear resistance or even for appearance's sake, color. The band gap (2.6 eV) and crystallite size (0.26 nm) were reported. Experimental findings indicated that the maximum specific capacitance reached 632.9 F/g at a scan rate of 100 mV/s, suggesting that these films may be suitable for supercapacitor applications.

It has been well established that the band gap of a material could greatly determine its potential in supercapacitor. Those with narrower band gaps have better electrical conductivities and rapid charge–discharge rates, which are suitable for HPSCs. On the other hand, narrower band gaps yield an increased power performance density, while a wider band gap might result in higher stability but with less energy density.

Even though several methods are used to fabricate electrodes thin film in case of supercapacitors but these two belong from different categories and have different natures. For large-area processing, the low-cost and simplicity possibly associated with SILAR method will be beneficial, while thermal deposition can provide better control on film thickness and crystal structures. In terms of thermal deposition, a source material is vaporized then deposited on the substrate. Typically, it is more costly and less flexible than chemical deposition method, as they use expensive equipment and high-vacuum conditions. As has been shown for many years, thermal deposition is a way to achieve very precise control of the specific capacitance and other important electrochemical properties.

3.8 Arsenic sulphide

Arsenic trisulfide (As_2S_3) is technically important materials due to their high transparency and excellent stability to corrosion. Several techniques have been used to grow As_2S_3 thin films. As_2S_3 films have been prepared by the solution gas interface technique, chemical bath deposition, and spin coating. However, the powdery nature of samples could be observed in EDTA complex acidic bath, while uniform and compact morphology for EDTA complex alkaline bath.

Thin films of arsenic sulphide have been prepared using different deposition techniques. The produced films may be used in photovoltaic devices, optical mass storage, hologram recording, and optoelectronic devices. The band gap measured was 2.6 eV, making it appropriate for use as absorber materials in thin films solar cells. High quality As_2S_3 films were deposited onto different substrates such as glass and silicon (111) wafer using As_2O_3 and $Na_2S_2O_3$ solution [36].

Silicon substrate was extensively applied for film forming because of its good electrical property, mechanical stability, and well-established fabrication technology. Their compatibility with electronic devices, high melting point and relatively low thermal expansivity makes them suitable for numerous thin film applications.

3.9 Nickel sulphide

Transition metal chalcogenides, like nickel sulfide are interesting materials from various aspects and particularly due to their unique electromagnetic property. The compositional, structural, and magnetic phase transition of nickel sulfide presents complex phenomena. A wide range of compositions were possible depending on the synthetic route and remain stable over different thermodynamic conditions. There are two phases of NiS: a low-temperature rhombohedral and a high-temperature hexagonal crystal structure. Also sulfur atom of Ssulf can be readily evolved to oxygen atoms under an oxygen atmosphere to create nickel oxide. Therefore, nickel sulfides show complicated behavior thus their properties need to be further elucidated with more detailed and systematic works.

In general metal sulfide nanoparticles have been synthesized via SILAR technique using sodium sulfide as a sulphur source. However, thiourea has been reported by one pot procedures. The growth of the NiS crystals consists of two periods: the nucleation process and the growth stage. The precursors for the final products were indicated above.

Nucleation and growth are two different stages in the process of phase transitions, for example such as crystallization, solidification or condensation. Nucleation is the first step of a phase transition in which a metastable phase creates stable clusters of a new phase. Next stage of the development is growth of these nuclei in bigger crystals. These nuclei need to pass over a barrier to be stable. And then when they get to a certain size, they can keep growing. Heterogeneous nucleation takes place at sites, such as impurities or the walls of vessels, with lower energy barriers.

Activation energy was 0.15 V for p-type NiS layers on single crystal Si (111) substrates [37]. It was noted that deposition cycle [38] greatly affected band gap values for NiS films (2.81-3.12 eV) and Ni_3S_4 samples (2.15-2.8eV). Hexagonal phase with a thickness of 350 nm for the films prepared using nickel nitrate and sodium sulfide at 27 °C [39]. C-H stretching modes could be identified through specific FTIR peaks such as 3480 and 1985 cm^{-1}.

3.10 Cobalt sulphide

The CoS films up to 25 cycles were uniform and highly adhered to the substrates. The films are black in colour. The thickness of the film was 0.3 μm for 25 cycles. All these wrinkled films detached from the substrates after 25 cycles of deposition, resulting from a generation of powdery films above dense films perfectly bound to the substrates. The influence of substrate on the properties of films was studied [40]. XRD investigations showed that an amorphous phase and polycrystalline phase could be observed by using glass and silicon (111) wafer, respectively.

CoS thin films were grown on stainless steel substrates for electrochemical testing. The charge-discharge cyclic voltammogram indicated that the capacitive behavior of the two crystalline and amorphous films does not have the typical rectangular shape. The hexagonal phase of films could be prepared using stainless steel [41]. Other results such as band gap (1.9 eV), optical conductivity ($1.77x10^{17}$ S^{-1}) and crystallite size (27.5 nm) were reported. Cobalt sulfide films may find use in optoelectronic and energy storage applications because of several distinctive characteristics. These films demonstrated 80% retention of charge capacity and exhibited a specific capacity (298.4 mAh/g).

Grayish black hue [42] transformed into a dark black shade as the deposition cycles increased from 35 to 115 during the experiment. Finally, researchers noted that the activation energy lowered (from 0.18 to 0.15 ev) as the films thickness increased from 201 nm to 513 nm. The number of defects and grain boundaries in a thin film can be decreased with the

increase in thickness. This will increase the uniformity and orderliness of the structure, making it easier for the charge carrier to go through and reduce the activation energy. This is a well-known phenomenon in many materials and is frequently associated with alterations of the microstructure and defects of the material with its thickness.

3.11 Indium sulphide

The strongest diffraction peak was (400) plane when $In(NO_3)_3$ was used. As-deposited films showed orange in color, however, changed to red after the annealing process. Crystalline structure could be observed in the presence of $InCl_3$ precursors. Outstanding photo response [43] was recorded in annealed samples (400 °C). Smooth morphology was found when indium sulfate was used in the presence of complexing agents such as TEA and hydrazine hydrae [44]. Band gap value was determined through absorption data and was estimated to be 2.7 eV.

The complexing agent for films is hydrazine hydrate ($N_2H_4 \cdot H_2O$). It plays a role in controlling the concentration of metal ions in the solution, thereby affecting the structure, morphology, and optical property of the film. Under normal conditions, the mean crystallite sizes increased with increase in the volume of hydrazine hydrate and decreased thereafter. This may refer to a high concentration of hydrazine hydrate, which results in increasing nucleation and crystallite growth. But at a further hydrazine hydrate concentration than the maximum concentration, there are more excess reagents, the concentration of reagent is higher than at the maximum concentration, and the crystallite size formed is low.

It has been observed that the lattice parameters, crystallites size and strain would change with concentration of hydrazine hydrate. The values of these parameters were found to increase with hydrazine hydrate volume, up to 80% from the concentration used, and again dropped. There is a significant reason that the lattice parameter increased up to a certain, then decreased, which is that the population of hydrazine hydrate is very effective about the internal strain of the chalcogenide materials.

When its volume is small, not much complexation with the metal ions occurs resulting in low amounts of the elemental sulfide being released into the solution. It causes orders of the structure to collapse and internal stress to be generated. Another possibility would be too high hydrazine hydrate, which causes too much complexity resulting in low ions of the metal again results in defects in the structure of the material.

3.12 $NiIn_2S_3$

ITO glass is commonly used as the substrate on which films are deposited since it is a conductive material that is both transparent and electrically conductive. ITO coated glass is a popular material for various applications, such as touch screen, display and solar cell. ITO is characteristic for the capability that several other thin films can be deposited on top of it, which can modulate or enhance its properties. ITO is used as a transparent electrode of solar cells, since it collects both the light and electricity under a presence of power generation layer while it is conducting. ITO is clear in the visible spectrum and can be used for applications where the light needs to fit through the substrate.

The In_2S_3Ni films were produced on glass coated with indium tin oxide (ITO) utilizing indium acetate, nickel chloride and sodium thiosulfate over 75 deposition cycles [45]. The ratio of sulfur to (In+Ni), and band gap decreased as the nickel concentration increased from 4% to 6%. Films are amorphous in character. It can be concluded according to the standard 2Θ and d values that the achieved film is cubic In_2S_3 structure. The substrate effect is significant in the films coated at Ni level between 0% and 4%.

The band gap shifts for the films can be interpreted in terms of band shrinkage effect. The non-constant band gap energy is attributed to the presence of Ni impurities on the In_2S_3 crystal, which provokes the shallow dopant level (donor level). This red shift of band gap may result from a rise in the carrier concentration, caused by doping with Ni. Furthermore, the red shift has been ascribed to a decrease in the concentration of S, which is found from the compositional analysis and results in a decrease in the optical energy gap for the In_2S_3:Ni thin films.

3.13 $CuAl_2S$

The thin film deposition process often uses ammonia (NH_3) as a complexing agent. The metal ions are complex with ammonia as ligand. It enables the ability to control the concentration of the metal ions in solution to avoid undesired precipitation and thus achieve reproducible, high quality thin films. In the absence of a complexing agent, the metal ions would chemically combine sulfide ions time and again, proceed to the production of a precipitate and rendering it impossible for a thin film to be deposited predetermined.

Ammonia and glass slide were used as complexing agent and substrate during the growth of films [46]. Film thickness (100.43 nm to 135.87 nm) was recorded in annealing conditions (100 to 250 °C, 1-2 hours). Monoclinic phase could be observed using copper sulphate, aluminium sulphate, and thiourea, 20 deposition cycles at pH 5.3. SEM analysis revealed that a rough surface is attributed to the presence of aluminum ion. These materials may be suitable for optoelectronic applications because of the linear decrease in reflectance value.

$CuAl_2S$ films have novel optical properties, such as controllable band gaps, which makes them promising candidates for optoelectronic devices. The composition, stoichiometry, and the microstructure of $CuAl_2S$ films influence the electrical conductivity, suggesting applications in electronic devices. These types of films are being investigated as a low-resistivity interconnect material for future generation semiconductor devices to replace the conventional copper interconnects with barrier layers. It is of great importance to tailor the properties of $CuAl_2S$ films for applications by well-controlled composition and microstructure.

3.14 Cadmium sulphide

High transmittance was observed for the films deposited on glass slide in the presence of Na_2S and $CdCl_2$. Stoichiometric composition was found when the immersion time and rinsing time were 20 seconds and 40 seconds, respectively [47]. XRD studies confirmed that polycrystalline phases in annealed films (250 °C, 30 minutes), respectively [48]. It was noticed that faster deposition growth could be seen when the glass slide substrate was modified with 3-mercaptopropyltrimethoxysilane [49]. Precursors such as thiourea and cadmium chloride were used to synthesize films [50]. It was noted that variations in crystallite size (12.44 to 14.65 nm) could be found when the deposition cycle was changed from 20 to 40 cycles. Polycrystalline phase with different sizes (20 to 80 nm) was

observed when the cadmium 2,4-pentanedionate, was used as precursor [51].

Homogeneous films were successfully prepared when the cycle was 125 cycles [52]. TEM studies confirmed that particle size was 23.5 nm when the cadmium acetate was selected as precursor [53]. FTIR (Fourier Transform Infrared) spectroscopy is the completive used to characterize thin film formation and properties. FTIR can help to draw some valuable inorganic-organic information and to locate how the infrared light interacts with the thin film. It is especially suitable for the characterization of thin films on a variety of substrates.

It was noted that thermal evaporation of CdS layer led to lower concentration in impurities induced in as-deposited layers with an improvement in the performance. This more crystalline structure in films often results in superior optoelectronic properties. A degree of preferred orientation may be displayed in the films, which can be advantageous for some applications such as solar cells. The resulting films are typically more uniform and compact, demonstrating roughness on lower surface. Existing Thermal evaporation is a traditional way to grow large-area thin films that are key for industrial applications [54].

Compared with thermal evaporation, the SILAR method results in smaller grain sizes. From the standpoint of performance, these SILAR-deposited films could have more scratches and other defects. Crystallinity may be a little lower than that obtained for thermally evaporated films. However, the reperformed SILAR deposition film prepared would be sometimes non-uniform with pinhole effect.

In general, the synthesized grains are monocrystalline and CdS layer which is prepared by close space sublimation method consist of single grain only. Consequently, the thickness of this layer is determined by the average CdS grain size. The high-resolution TEM image displays good crystallinity. There were a few aberrations that could be seen within the crystal. The deposited CdS by sputtering is bigger in grains and is crystalline. Although electro deposition method is also a solution method at low temperature, the CdS made by electro deposition exhibits far better crystallinity than SILAR deposited CdS. Since the growth mechanism by electro deposition method may be thought because electrodeposition of CdS yields such as an epitaxial film from specific substrate. This is due to the ion and chemical reaction that can be controlled in a solution.

Vacuum deposition methods could deliver more effective thin films than SILAR, specifically in solar cells. It is largely attributed to the better quality of the film, such as a higher crystallinity, a larger grain size, and denser morphology that can be obtained in-vacuum deposition process. With the use of vacuum depositions, researchers can deposit high-purity films from high purity source materials and, this in turn can result in a film with better quality and performance.

Vacuum based deposition techniques have better ability to control the film thickness and composition compared to SILAR, which can be critical for optimizing device performance. Hexagonal phase formation was facilitated by vacuum evaporation while SILAR technique yielded films with mixed hexagonal and cubic structure. Results showed that the band gap energy of the vacuum deposited CdS films was greater than SILAR deposited films.

3.15 Copper sulphide

Thin films of CuS have been deposited on different substrates, such as glass slides and silicon (111) wafers, utilizing a solution of thiourea and copper sulphate [55]. Highly polycrystalline covellite films have been synthesized by using a Na_2S and $CuSO_4$ solution [56]. On the other hand, cupric sulphate and sodium thiosulfate were selected as precursors. It was noticed that significantly different morphologies such as irregular microspheres, and flower-shaped grains could be observed in different deposition cycles. The overall outcomes showed a significant absorbance value within the visible spectrum [57]. The average transmittance exceeded 70% in the UV-visible NIR range for all films, demonstrating their suitability as optical coating materials [58].

Thin film materials are materials deposited in thin layers on surfaces of optical elements to modify the interaction of light with the surface. Such materials are commonly metals (aluminum, silver and gold) or dielectrics (oxides, fluorides). These materials are selected for optical properties and particular use, for example anti-reflection, high-reflectance or filtering.

The hexamethyltetraammine serves as a complex agent by chelating with metal ions. Four nitrogen atoms with a lone pair of electrons on each (electron-donating) are capable of binding metal ions. This characteristic makes hexamethylenetetramine applicable in diverse reactions such as the synthesis of metal complexes, precipitation of metal ions, and a precursor to catalyst. It may also serve as an outer sphere modulator for the metal complex inner coordination sphere.

The Cu_2S films were synthesized with various complexing agents [59] such as hexamethyltetraammine and ammonia solution in specific conditions. Raman spectroscopy and XPS studies revealed that there was a significant peak at 472 cm^{-1} with no additional impurities. The films synthesized with ammonia achieved maximum specific capacitance of 765 F/g. It was noted that thin films made with ammonia (95%) demonstrated superior stability over 2000 cycles when compared to hexa-methyltetrammine (93%). According to the HRTEM images, a thicker structure (d-spacing value was 3.012Å and a nanotube structure (d-spacing value was 3.105Å) were prepared using ammonia and hexamethyltetrammine, respectively.

High Resolution Transmission Electron Microscopy is a powerful imaging method for the atomic resolution of materials. It provides information about the number of atoms in a sample, crystal structures, grain size and local fluctuations in structure and chemical composition. HRTEM is an advanced type of transmission electron microscopy that provides the capability for ultimate magnification like which an atom can be resolved.

3.16 Zinc sulphide

FTO-coated glass offers a cheaper alternative to ITO-coated glass as a conductive glass. It is a conductive function glass, which is adhered to a transparent FTO conductive layer by physical bonding or a chemical bonding process. It has surface resistivities of less than 7 to 15 ohms. It is a cost-effective alternative to ITO-coated glass for solar cell research and development. It's an inventive uncoated, single-side glass with a tetragonal structure. The present invention provides a green coating process in which the amount of substance used is drastically reduced, the coating becomes thinner, and the

coating weight becomes more uniform and without leaking, and maintenance is minimized.

There are three peaks [60] that could be identified (413, 480 and 525 nm) for the films prepared using thiourea, zinc acetate and complexing agent (ammonium hydroxide). Sample with thickness of 1.43 μm was prepared on FTO glass [61], showed about 0.1% efficacy.

Nanostructured films have been grown by using sodium sulfide, zinc chloride, and triethanolamine [62]. When the temperature increases, the amorphous phase has been transformed into crystalline phase. XRD studies exhibited that crystallite size and thickness were 12 nm and 1 μm, respectively when the ammonia serves as complexing agent [63]. Growth rate was observed to be 0.23 nm/cycle when the substrate was GaAs [64]. XRD studies displayed that the strongest peak at 2θ=29° in specific thickness (136 nm). On the other hand, the growth rate was 0.13-0.27 nm/cycle when the substrate was soda lime glass [65]. Refractive indices were 1.95-2.23 when the complexing agent was TEA solution, and immersion time was 20 seconds.

Soda-lime glass is the most common and inexpensive substrate for thin film deposition, but its constituent materials can influence thin film properties and device performance, especially at elevated temperatures. Sodium ions in the glass can migrate into the thin film leading to lower photo efficiency, device delamination and shunt paths. Pinholes are short circuit generating mechanisms (shunt paths) that can be introduced into electronic devices through defects in the thin film, often caused by sodium diffusion. However, methods such as photolithography and proton exchange can help to reduce these problems by providing a diffusion barrier layer, or by inhibiting sodium migration.

In the case of ZnS thin films, they can be prepared via spray pyrolysis and SILAR methods. In the case of spraying a solution of zinc and sulfur precursors onto a heated substrate or treating the substrate in sequential baths of chemical reaction solutions, as in SILAR. Each method presents its pros and cons, being that spray pyrolysis is widely used for large area depositions, while SILAR based technique remains as the simplest route for the growth of good quality films at lower temperatures.

3.17 Copper tin sulphide

In the thin film growth process, Ethylenediaminetetraacetic acid (EDTA) is employed to suppress the deposition rate and high-quality thickness. It's a chelating agent which binds to metal ions and liberates them gradually for more controlled film growth. EDTA also can affect the structure, crystalline, and optical properties of the film. Inhibiting the release of metal ions, EDTA will favor larger grain sizes and a more complete coverage of the surface. On other cases, EDTA may assist in suppressing the presence of unwanted phases in the film.

Cu-Sn-S films have been prepared in specific conditions. Orthorhombic (Cu_4SnS_4) and cubic (Cu_2SnS_3) have been synthesized in H_2S atmosphere and a mixture of nitrogen and sulfur vapors, respectively [66]. Stainless steel substrates have been used to produce n-type Cu_2SnS_3 films using EDTA solution [67]. The XPS studies emphasized the +1 for copper and +4 for tin, respectively. XRD and SEM techniques were employed for the characterization purposes, results showed triclinic phase and spherical grains, respectively.

Cu_2SnS_3 films were subjected to annealing at 350 °C for 1 hour [68]. Annealed samples showed unique properties such as polycrystalline structure, smaller band gap value (1.21 eV) and rich in copper concentration. Uniform morphology and dark coloration could be observed when the substrate was indium doped tin oxide glass [69]. XPS studies confirmed that the presence of Cu^{+1}, Sn^{4+} and S^{2-} in the Cu_2SnS_3 annealed films. Photovoltaic properties were investigated, fill factor and efficiency were 30% and 0.11%, respectively, in ITO/CTS/$LiClO_4$/graphite solar cells.

Annealing is applied as a process step to optimize thin film microstructure and associated opto-electronic properties. That means not just heating the film to a certain temperature but also keeping it that hot for a particular amount of time before cooling it, often to room temperature. This post-treatment may help to increase the crystallinity of the films, decreasing the defect level and modifying the surface morphology of the film, which directly affects the electrical, optical, and mechanical characteristics.

3.18 Tin sulphide

When silicon (111) was selected as the substrate, the prepared n-type SnS_2 films showed a band gap of 2.6 eV [70]. When the glass slide was used as substrate, the band gap reduces with increasing the concentration of complexing agent (TEA) concentration [71]. SnS films have been grown using ammonium sulfate and stannous chloride [72]. When the Na_2S and $SnSO_4$ solution [73] were used as precursors, thickness of 0.2 μm could be observed for the samples deposited onto ITO glass slides. The photoluminescence spectrum exhibited two peaks such as 680 nm and 825 nm. Raman studies highlighted that SnS phase could be observed when $SnCl_2$ and Na_2S were used as precursors via 40 deposition cycles [74]. It was noticed that the band gap decreases by increasing the concentration of complexing agent such as ethylene diamine tetra acetic acid (0.05 M to 0.2 M).

The SILAR approach was used to synthesize tin sulfide nanoparticles by varying the capping agent (L-ascorbic acid) dosage. From the temperature range of 200 to 400 °C, researchers annealed the samples under an inert atmosphere to increase crystallinity of the films, and it is found that the as-deposited and annealed tin sulfide thin films have a strong adhesion to the substrate. It was also observed that, as the annealing temperature was higher, the films that were produced were smoother and thinner. As regards L-ascorbic acid amount, it does not influence phase composition. But it seems that a large quantity of ascorbic acid is beneficial to crystallinity structure.

In Raman (figure 1), researchers have found one broad peak at about 314 cm^{-1} in sample annealed at 400 °C which indicate the presence of the only broad peak which might corresponds to the SnS_2 nature [75], and an increase in peak due to SnS_2 and decrease in the peak due to SnS. Most likely, high temperature annealing leads to the transformation of SnS to SnS_2.

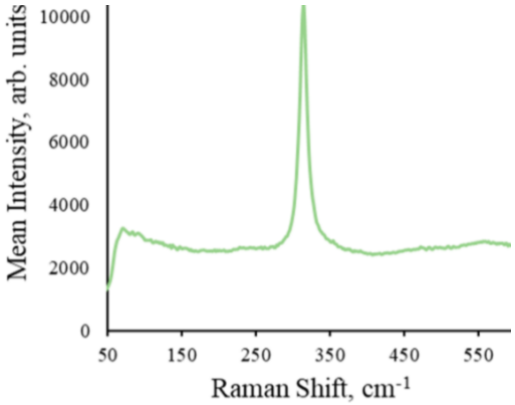

Fig. 1. Raman studies of films (400 °C, 0.8 g L-ascorbic acid [75]).

The thin films were reported to be multiphase with Sn(II) larger at lower temperatures. Tin sulfide annealed at 300 °C and 350 °C will be the most active in the current peaks in relation to potential applied. Instead, this observation could be linked to the fact that in these films, tin has two main oxidation states (+2 and +4). Oxidation diversity is often an important factor influencing the electrochemical properties of pseudocapacitors.

SnS has a layered structure that is beneficial for ion intercalation as such it shows improved capacitive behavior. The thickness of the films becomes lower as the temperature goes upwards. Researchers attribute this fact to the elimination of vesicles of ascorbic acid from the samples and more compact packing of the structure. In addition to, these crystallites can be arranged near a surface by employing a smoother one.

The synthesis techniques of tin sulfide thin films using pulsed laser deposition (PLD) and SILAR technique has a capability of manipulating the properties of film according to the deposition and growth conditions. While the pulsed laser deposition enables higher growth rates and better stoichiometry control, SILAR is a simple cost-effective solution-based method. The method produces a film with orthorhombic structure, which is desirable for other thin-film applications, such as thin-film solar cells.

Broadly, PLD involves the usage of high-power laser pulses to ablate material from a target resulting in a plasma plume which deposits the material on the substrate. Typically, the deposition rate is roughly 0.1 nm per pulse and the repetition frequencies are between 1 Hz and 100 Hz. The real advantages of PLD are much higher growth rate as compared to some conventional deposition techniques. Since PLD can be tailored for fast growth with some liquid constituents, this may assist in developing films that contain high performance pinning sites.

3.19 Copper zinc tin sulfide

Copper zinc tin sulfide (CZTS) is a quaternary semiconductor compound that consists of copper, zinc, tin, and sulfur. It has received much attention as one of the candidates to replace indium based solar cells for thin-film photovoltaics because of the earth-abundance, nontoxicity and low cost of the elements. In addition, CZTS has attractive features such as appropriate bandgap for solar energy conversion and high absorption coefficient.

Glass slide was used as substrate [76] to prepare uniform tetragonal films. The values for resistivity ($1.51x10^2$ Ωcm), band gap (1.5 eV), mobility (0.32 $cm^2/V.s$), absorption coefficients (10^4 cm^{-1}) and carrier density ($1.28x10^{17}cm^{-3}$) were reported. Raman spectroscopy showed two significant peaks at 287 and 336 cm^{-1}, respectively [77]. When the deposition cycle was increased, it was noted that grain size will be enhanced also [78]. Fluorine doped tin oxide glass was utilized as substate to form non-toxic materials [79]. Photovoltaic characteristics including fill factor (0.62), efficiency (0.396%), open circuit voltage (390 mV) and short circuit current (636.9 μA/cm^2) were reported.

In many deposition methods grain size increases with deposition cycle number. This development is sometimes attributed to the enhanced diffusion of atoms or groups of atoms on the deposition face such that they can combine to build up larger crystals. This relationship is, however, generally not linear and can be affected by other parameters such as deposition temperature, kind of precursor and the exact way of deposition.

During the growth with the increasing number of deposition cycles deposit starts to pile up. This may facilitate higher surface temperatures or higher diffusion rates, resulting in more mobile atoms which can access lower energy configurations. Epitaxy The epitaxy is a situation where the deposited material crystal structure is adopted from the underlying substrate. This may result in anisotropic growth and the development of large grains.

3.20 Silver sulphide

Fluorine doped tin oxide glass was selected as substrate to synthesize n-type Ag_2S films. The photoelectrochemical investigations showed that significant series resistance resulted in lower efficiency value. Sample with thickness of 299 nm could be found [80] in specific conditions. Homogeneous morphology and the strongest diffraction peak could be observed in (100) plane. Sample with the thickness of 0.22 μm was fabricated using silver nitrate, thiourea at 27 °C. XRD data confirmed the recrystallization process could be found din annealed samples. It was noted that electrical resistivity (2.58 to 1.99 $x10^4$ Ωcm) decreased as temperature increased from 373 K to 573K [81].

Deposition of Ag_2S films on glass slides in the presence of ammonia at 40 °C was reported [82]. The prepared films showed a monoclinic phase, and a favored orientation related to the (120) plane. Thin films were prepared using thiourea and silver nitrate with 30 deposition cycles, at 27 °C, a rinsing duration of 10 seconds, and an immersion duration of 15 seconds [83]. It was noted that film thickness was 135 nm, suitable for sensitized solar cells because of their nontoxic materials [84], and outstanding short circuit current [85].

The higher the short-circuit current of a solar cell, the larger the fill factor and open-circuit voltage, all things being equal, and hence the higher the possible power output and efficiency. But it's important to remember that short-circuit condition (when there is no voltage) is not the way solar cells are supposed to be used. A higher short-circuit current is good, but it's ultimately open-circuit voltage and how well a cell can retain that voltage under load that make a difference to the power and efficiency of the cell.

3.21 Sb_2S_3

Sb_2S_3 is classified as a group V-VI material. It features a consistent orthorhombic crystal arrangement. It displays n-type electrical conductivity with large band gaps and is the most promising candidate to produce quantum dot solar sensitized cells. Sb_2S_3 is non-toxic by nature and exists as a highly stable phase. The melting point temperature is 550 °C. Crystals of these materials displayed an orthorhombic form and are categorized in the Pnma (#62) space group. It may be used in microwave equipment, TV cameras, switching apparatus, and a range of optoelectronic instruments. It is a significant material due to its photosensitive and thermoelectric properties.

Non-stoichiometric Sb_2S_3 films could be prepared using glass slide as the substrate [86]. Raman spectroscopy confirmed that two major peaks (250 and 300 cm^{-1}) could be found in orthorhombic phase samples. Glass slide was used to fabricate films using antimony trioxide and sodium thiosulfate [87]. When the deposition cycle increases, it was noted that film thickness also increased. Other results such as band gap (1.8 eV), resistivity (107 Ωcm) and activation energy (0.14 eV).

Surfactants refer to compounds with an amphiphilic radical, such as hydrophilic radical and hydrophobic radical, in their molecules. Thus, they can enhance the ability of a solid to be wet. The reactants and the substrate are $Mn(CH_3COO)_2$, $Co(NO_3)_2$, Na_2S, and foam nickel, respectively. During the formation of films, anionic and cationic surfactants were identified as SDS (sodium dodecyl sulfate) and CTAB (cetyl trimethyl ammonium bromide). The assisted surfactant increased the loading of MnCoS in large quantity, which was deposited homogeneously of the deposited layer. The capacity was also improved greatly, and they showed very good electrochemical performance.

The surfactants can be adsorbed onto the nickel foam spontaneously because they make the surface free energy reduce and change the wetting property of the surface and the electronic property, thus can increase the activity of the catalyst. In TEM images [88], it was noted that the particle size was 20 nm in MnCoS-CTAB composite (figure 2a). In HRTEM findings, lattice fringes of 0.276 and 0.305 nm, belong to the CoS (200) and MnS (200) plane, respectively (figure 2b). The small resistances are good for fast electron transfer and ion diffusion across electrode materials. This can also be used to account for the highest specific capacitance of MnCoS-CTAB. The specific capacity of MnCoS-CTAB in the end can reach 2029.8 F/g, which was superior to that of MnCoS-SDS of 1500.2 F/g, and was much higher than that of MnCoS-H_2O being 950.4 F/g. In addition, the MnCoS-CTAB material also exhibited long-term cyclic stability; the specific capacity could reach a retention rate of 71% after 1000 cycles, suggesting grand application prospects.

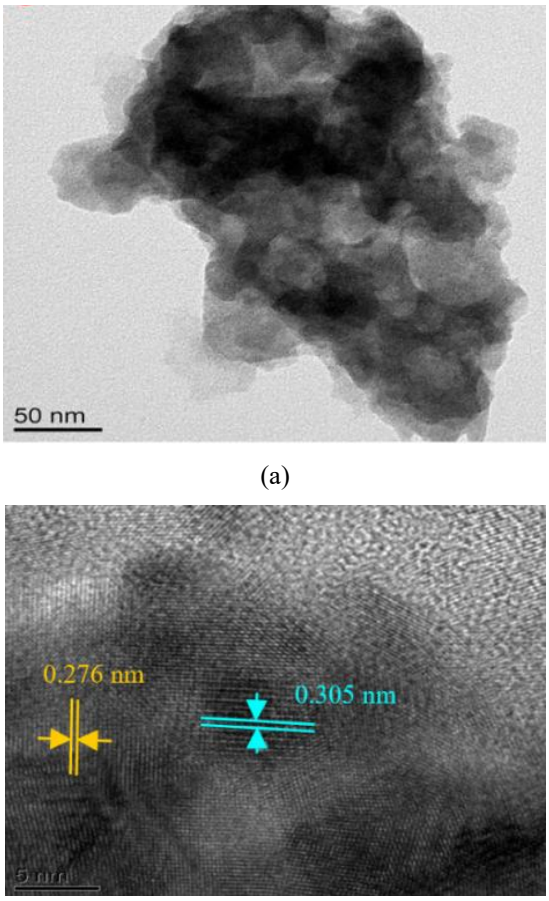

Fig. 2. (a) TEM images (b) HRTEM images of MnCoS-CTAB [88]

4. Comparison of Silar Method with Other Deposition Techniques

Methods to deposit thin films on a substrate can be classified into two broad categories, namely the physical and chemical methods. Physical vapor deposition (PVD) and chemical vapor deposition (CVD), the acronyms stand for physical vapor deposition, deposited through a physical process such as evaporation or sputtering onto the substrate; chemical vapor deposition relies on chemical reactions between gaseous precursors that form a solid film on the substrate.

SILAR and chemical bath deposition are chemical methods for thin-film deposition. These result from chemical reactions in liquid solution of the precursor, that produce a thin film on the substrate.

In the chemical bath deposition method, the growth of thin film metal chalcogenides films from a solution involves immersing a substrate into the bath of the appropriate ions to produce the desired thin film [89]. As ions respond and deposit, the film grows through heterogeneous nucleation on the substrate surface.

As a result of the film growth by chemical bath deposition method, thin films have shown better grain structure and crystallinity has also been better than that observed in SILAR-deposited films where the initially grown metal sulfide layer acts as seed layer for further development of film and particles start stacking over one another with c-axis being preferred

direction for its growth. In heterogenous nucleation, single ions and clusters particles can attach to the surface. The energy needed to generate an interface between the nuclei (stable clusters of ions and molecules) and solid substrate, necessary for due to cessation nucleation will generally be lower than that required for homogeneous nucleation (in the absence of such interface). As a result, the heterogeneous nucleation is energetically favorable to homogeneous nucleation. The nucleation grows to particles during the immersion of substrate into a reaction bath and then the particles are forced onto the substrate surface. So, there is no preferential direction of thin film growth obtained through SILAR method.

In general, resistivity was decreased with increase temperature which represents the semiconducting behavior for thin films. The resistivity is lower in films deposited by chemical bath deposition compared to SILAR because vertical nanorods form and larger grain size allows pathway for electron conduction but in the case of nanograins formed by SILAR-deposited, electronic motion is hampered due to large no. of grain boundaries hence resistivity increases. Similarly, large quantity of chemisorbed oxygen species is trapped at grain boundaries due to electron trapping nature in SILAR grown films contributed to the increment of surface resistance as well.

The films prepared by chemical bath deposition were comparatively highly porous and rough in nature than those of deposits obtained by SILAR. The presence of vertically oriented nanorods retained air inside the gaps between the rods and water droplet, higher interfacial surface energy was raised as a result so that water (partially) soaked in the film making contact angles bigger which indicates hydrophobic nature. As in the case of rod-like morphology, interfacial surface energy is lower than granular structure due to which contact angle shows slight decrease.

Electrodeposition method is an electrochemical process which involves the deposit of a thin layer of metal or other material on a conducting surface via electricity [90]. Basically, it is a type of electrolysis, where metal ions are reduced in solution and deposited at the cathode. Sputtering is one of the physical vapor depositions processes in which high energy ions are bombarded on target material and it results in ejection of atoms or molecules from a source [91], deposition onto substrate manufacture with solid state thin film.

The process of vacuum deposition is a coating technique that uses physical vapor deposition and chemical vapor deposition methods at a lower atmospheric pressure or within a higher vacuum environment. It is employed to negotiate the electrical, optical or mechanical characteristics of materials and it has numerous applications in fields such as microelectronics and optics.

Thermal evaporation is a physical vapor deposition method used to produce thin films. It consists of heating a material to evaporate it in vacuum and deposit the vapors on a substrate where they condense returning growth by layers [92], forming the film. This step is applied in many applications including the fabrication of coatings for optics, electronics, and other materials. This is carried out in a vacuum chamber, as gas molecules would otherwise interfere with the evaporated material. The source material may be solid at room temperature or liquid, but when heated to a high temperature the material vaporizes. That source material is heated up, which causes it to either melt (if a solid) or sublimate (if it goes straight from solid to gas). The vaporized material then travels through the vacuum and condensed onto a cooler substrate which it bonds to to produce a thin film.

Spray pyrolysis is a method of producing thin films and nanoparticles from the precursor solution by spraying it onto a heated substrate to evaporate the solvent [93], with consequent decomposition and reaction of chemical compounds defined in this process to form a solid film or powder. The technique is both versatile and relatively straightforward, particularly conducive to the synthesis of metal oxides.

Overall, researchers were keen to point out that all methods of deposition have benefits and disadvantages (Table 2). The best way, however, is selection of deposition method depending on the application of products and characteristics of the materials to be synthesized as well as goals

Table 2. Disadvantages of several depsotion methods

Deposition method	Disadvantages
Electro deposition	Unfit for large scale manufacturing
Spray pyrolysis	Very complicated process
Radio frequency sputtering	Low depositon rate
Molecular beam epitaxy	Very expensive
Sol gel method	High cost
Vacuum depostion	High cost
Hydrothermal method	Expensive autoclaves
Magnetron sputtering	Low depostion rate
Chemical bath deposition	Wastage of chemical solution

5. CONCLUSION

The thin layers of metal sulfide have been successfully deposited on various substrates via SILAR deposition technique. These materials can be utilized in sensor, solar cells, and supercapacitors. Higher growth rate generally leads to thicker film as film collects material faster after some time. The achieved film reveals, annealing after the deposition to be beneficial for the quality of the film; hence roughness decreases and the crystalline nature of the ZnS is improved. High quality films are obtained by optimizing certain experimental conditions like deposition cycles, complexing agent, immersion time, rinsing time, annealing temperature and concentration of solution.

ACKNOWLEDGEMENT

This research work was supported by INTI International University, Malaysia.

REFERENCES

[1] M. Wang, F. Yu and Y. Wen, “Co3O4 spinel film by atomic layer deposition on ferritic stainless steel SUS430” J. Eur. Ceram. Soc., 2025, doi: https://doi.org/10.1016/j.jeurceramsoc.2025.117711.

[2] P. Lopez, G. Diaz, L. Jose and D. Joel, “Effect of selenium doping on the deposition and properties of cadmium sulfide thin films grown by a chemical bath deposition technique,” Opt. Mater., 2025, doi: https://doi.org/10.1016/j.optmat.2025.117087.

[3] M. Yu, Q. Lv, T. Feng and H. Xu, "Lead selenide thin films: From first principles to in situ crystalline thin film growth by thermal evaporation," Thin Solid Films, 2025, doi: https://doi.org/10.1016/j.tsf.2025.140661.

[4] G. Luis, L. Jose, A. Cesar and E. Haro, "Experimental and computational investigation on the surface plasmon resonance of copper thin-films produced via pulsed laser deposition," Results Opt., 2025, doi: https://doi.org/10.1016/j.rio.2025.100803.

[5] F. Haidar, A. Pradel, Y. Chen and R. Marie, "Deposition of Sb2Se3 thin films on Pt substrate via electro-chemical atomic layer epitaxy (EC-ALE)," J. Electroanal. Chem., 2020, doi: https://doi.org/10.1016/j.jelechem.2020.114774.

[6] A. Albin, S. Ganesh, P. Poornesh and I. Kityk, "Influence of electron beam irradiation on nonlinear optical properties of Al doped ZnO thin films for optoelectronic device applications in the cw laser regime," Opt. Mater., 2016, doi: https://doi.org/10.1016/j.optmat.2016.09.053.

[7] J. Men, J. Zhang, Y. Li and X. Xie, "Low-temperature preparation of high electrical conductivity amorphous compact Zn-doped TiO2 thin films via vacuum ultraviolet for high efficient solar cells," J. Solid State Chem., 2025, doi: https://doi.org/10.1016/j.jssc.2025.125302.

[8] M. Radaf and H. Zahrani, "Structural, electrical, linear and nonlinear optical analysis of the innovative n-type ZnV2O4 thin films synthesized by spray pyrolysis," Opt. Mater., 2025, https://doi.org/10.1016/j.optmat.2025.116669.

[9] R. Angel, H. Farias and W. De, "P-type ZnO:N thin films deposited at room temperature on different substrates for p-channel thin film transistor fabrication," Vacuum, 2025, doi: https://doi.org/10.1016/j.vacuum.2024.113926.

[10] S. Padwal, R. Wagh and T. Jivan, "Integrated synthesis and comprehensive characterization of TiO2/AgBi2S3 ternary thin films via SILAR method," Heliyon, 2023, doi: https://doi.org/10.1016/j.heliyon.2023.e23106.

[11] Z. Tseng, Y. Chang, C. Lin and C. Huang, "Highly stable flexible ozone gas sensors using Mn3O4 nanoparticles-decorated IGZO thin films through the SILAR method," Ceram. Int., 2024, doi: https://doi.org/10.1016/j.ceramint.2024.05.168.

[12] G. Emna, N. Khemiri and M. Kanzari, "Silver doping induced modifications in the physical properties of indium sulfide powders and thin films," J. Alloys Compds., 2025, doi: https://doi.org/10.1016/j.jallcom.2025.179625.

[13] J. Damisa and J. Emegha, "Growth and Optical Analysis of Cobalt Tin Sulphide Thin Films using SILAR Technique," Niger. Res. J. Eng. Environ. Sci. 2021, vol. 6, pp. 642-648.

[14] W. Ying, J. Chen, L. Jiang and F. Liu, "Characterization of Bi2S3 thin films synthesized by an improved successive ionic layer adsorption and reaction (SILAR) method," Mater. Lett., 2017, vol. 209, pp. 479-482.

[15] M. Bouachri, H. Farri, M. Taibi and M. Beraich, "Influence of cycle numbers on optical parameters of nanostructured Bi2S3 thin films using SILAR method for solar cells light harvesting," Materialia, 2021, doi: https://doi.org/10.1016/j.mtla.2021.101242.

[16] D. Dipalee, S. Shaeed, S. Farha and R. Birajdar, "Enhancement of photosensitivity by annealing in Bi2S3 thin films grown using SILAR method," Compos. B Eng. 2013, vol. 46, pp. 1-6.

[17] S. Shrikant, A. Jyotsna and R. Babasaheb, "SILAR deposited Bi2S3 thin film towards electrochemical supercapacitor," Phys. E. 2017, vol. 87, pp. 209-212.

[18] K. Mageshwari and R. Sathyamoorthy, "Nanocrystalline Bi2S3 thin films grown by thio-glycolic acid mediated successive ionic layer adsorption and reaction (SILAR) technique," Mater. Sci. Semicond. Process., 2013, vol. 16, pp. 43-50.

[19] U. Ubale, R. Raut and H. Bhosale, "Electrical and optical properties of Bi2S3 thin films deposited by successive ionic layer adsorption and reaction (SILAR) method," Mater. Chem. Phys., 2008, vol. 110, pp. 180-185.

[20] S. Sartale and C. Lokhande, "Studies on large area (~50 cm2) MoS2 thin films deposited using successive ionic layer adsorption and reaction (SILAR) method," Mater. Chem. Phys. 2001, vol. 71, pp. 94-97.

[21] N. Akshay and S. Sartale, "Modified chemical route for deposition of molybdenum disulphide thin films," AIP Proc., 2014, doi: https://doi.org/10.1063/1.4872808.

[22] K. Tapio, L. Seppo and I. Jarkko, "Growth of strongly orientated lead sulfide thin films by successive ionic layer adsorption and reaction (SILAR) technique," J. Mater. Chem. 1996, vol. 6, pp. 161-164.

[23] J. Puiso, G. Laukaitis, M. Leskela and S. Lindroos, "Growth of PbS thin films on silicon substrate by SILAR technique," Thin Solid Films, 2002, vol. 403-404, pp. 457-461.

[24] Y. Gulen, "Characteristics of Ba-Doped PbS Thin Films Prepared by the SILAR Method," Acta. Phys. Polonica A., 2014, vol. 126, pp. 763-767.

[25] E. Guneri, F. Gode and S. Cevik, "Influence of grain size on structural and optic properties of PbS thin films produced by SILAR method," Thin Solid Films, 2015, vol. 589, pp. 578-583.

[26] K. Preetha, K. Murali and A. Ragina, "Effect of cationic precursor pH on optical and transport properties of SILAR deposited nano crystalline PbS thin films," Curr. Appl. Phys., 2012, vol. 12, pp. 53-59.

[27] V. Vishal, R. Devan, S. Pawar and S. Namdev, "Chemically synthesized PbS nanoparticulate thin films for a rapid NO2 gas sensor," Mater. Sci. Poland, 2016, doi: https://doi.org/10.1515/msp-2016-0001.

[28] B. Mahesari and M. Dhanam, "Optimization of deposition temperature of SILAR Cu-rich CuInS2 thin films," Mater. Sci. Poland, 2013, vol. 31, pp. 193-200.

[29] P. Wei, J. Gong, C. Ge and J. Li, "Preparation and Properties of CuInS2 Thin-Film by Successive Ionic Layer Adsorption and Reaction (SILAR) Method," Key Eng. Mater. 2005, doi: https://doi.org/10.4028/www.scientific.net/KEM.280-283.877.

[30] X. Xueqing, Q. Wan, C. Luan and F. Mei, "Fabrication of CuInS2-Sensitized Solar Cells via an Improved SILAR Process and Its Interface Electron Recombination," Appl. Mater. Interfaces. 2013, vol. 5, pp. 10605-10613.

[31] X. Fanghong, S. Yong, Q. Zhao and C. Li, "Effects of hydrothermal annealing on characteristics of CuInS2 thin films by SILAR method," Appl. Surf. Sci., 2012, vol. 258, pp. 7465-7469.

[32] J. Zhengguo, S. Yong, C. Li and J. Qiu, "Effect of [Cu]/[In] ratio on properties of CuInS2 thin films prepared by successive ionic layer absorption and reaction method," Appl. Surf. Sci., 2006, vol. 252, pp. 3737-3743.

[33] K. Manikandan, P. Mani, S. Dilip and H. Fermi, "Effect of complexing agent TEA: The structural, morphological, topographical and optical properties of FexSx nano thin films deposited by SILAR technique," Appl. Surf. Sci., 2014, vol. 288, pp. 76-82.

[34] M. Yildirim, Y. Tuna, A. Ates and I. Cavanmirza, "Chemically synthesis and characterization of MnS thin films by SILAR method," Chem. Phys. Lett., 2016, vol. 647, pp. 73-78.

[35] A. Admuthe, S. Sambaji, K. Susmita and N. Ganesh, "Synthesis and Characterization of MnS Thin Film at Room Temperature for Supercapacitor Application," Macromol. Symp., 2020, doi: https://doi.org/10.1002/masy.202000186.

[36] D. Sartale and C. Lokhande, "Preparation and characterization of As2S3 thin films deposited using successive ionic layer adsorption and reaction (SILAR) method," Mater. Res. Bull., 2000, vol. 35, pp. 1345-1353.

[37] D. Sartale and C. Lokhande, "Preparation and characterization of nickel sulphide thin films using successive ionic layer adsorption and reaction (SILAR) method," Mater. Chem. Phys., 2001, vol. 72, pp. 101-104.

[38] O. Ofeliya, A. Azizov, B. Mustafa and M. Abel, "β-NiS and Ni3S4 nanostructures: Fabrication and characterization," Mater. Res. Bull., 2016, vol. 75, pp. 155-161.

[39] D. Sathya, "NiS thin films for solar cell application by successive ionic layer adsorption and reaction (SILAR) method," GIS Sci. J., 2022, vol. 9, pp. 89-95.

[40] D. Sartale and C. Lokhande, "Deposition of cobalt sulphide thin films by successive ionic layer adsorption and reaction (SILAR) method and their characterization," Indian J. Pure Appl. Phys., 2000, vol. 38, pp. 48-52.

[41] O. Kester, N. Blessing, A. Agbogu and C. Nwanya, "The effect of deposition cycles on intrinsic and electrochemical properties of metallic cobalt sulfide by Simple chemical route," Mater. Sci. Semicond. Process. 2019, vol. 101, pp. 16-27.

[42] A. Mitkari and U. Ubale, "Thickness Dependent Physical Properties of SILAR Deposited Nanostructured CoS Thin Films," ES Mater. Manuf., 2019, vol. 5, pp. 49-56.

[43] R. Anita, J. Teny and K. Sudha, "Structural and Optical Properties of Indium Sulfide Thin Films Prepared by Silar Technique," Open Condens. Matter Phys. J., 2009, vol. 2, pp. 9-14.

[44] M. Pathan, S. Han, T. Seth and S. Kulkarni, "Some studies on successive ionic layer adsorption and reaction (SILAR) grown indium sulphide thin films," Mater. Res. Bull., 2005, vol. 40, pp. 1018-1023.

[45] G. Fatma and U. Serdar, "Nickel doping effect on the structural and optical properties of indium sulfide thin films by SILAR," Open Chem., 2018, vol. 16, pp. 757-762.

[46] O. Joseph, E. Ngozi and N. Kelechi, "Optical Properties of CuAl2S Alloyed Thin Films Prepared Using Enhanced Successive Ionic Layer Adsorption and Reaction Method," Int. J. Res. Innov. Appl. Sci., 2021, vol. 6, pp. 95-99.

[47] B. Fouad, A. Raidou and T. Sall, "Structural and optical properties of CdS thin films prepared by SILAR method," 2013 International Renewable and Sustainable Energy Conference (IRSEC), 7-9 March 2013, Ouarzazate, Morocco, pp. 73-77.

[48] J. Dipalee, S. Shaeed, S. Farha and R. Birajdar, "Effect of annealing on structural and optoelectronic properties of CdS thin film by SILAR method," Adv. Appl. Sci. Res., 2011, vol. 2, pp. 417-425.

[49] S. Hua and J. Mu, "SILAR Deposition of CdS Thin Films on Glass Substrates Modified with 3-Mercaptopropyltrimethoxysilane," J. Dispers. Sci. Technol., 2005, https://doi.org/10.1081/DIS-200063026.

[50] O. Kester, M. Tochukwu and I. Kenneth, "Influence of Dip Cycles on the Structural, Optical and Morphological Properties of CdS-SILAR Deposited Thin Films," J. NanoSci. NanoEng. Appl., 2016, vol. 6, pp. 19-26.

[51] T. Loreta, S. Birute, Z. Albina and N. Leonas, "Investigation of CdS Thin Films Deposition by the SILAR Method Using Cd(II) Organic Salt as Precursor," ECS Meeting Abstr., 2014, doi: https://doi.org/10.1149/MA2014-02/15/837.

[52] K. Garadkar, A. Patil, P. Krake and P. Hankare, "Characterization of CdS thin films synthesized by SILAR method at room temperature," Arch. Appl. Sci. Res., 2010, vol. 2, pp. 429-437.

[53] P. Mitra, M. Ayan and P. Protim, "Synthesis of Nanocrystalline CdS by SILAR and Their Characterization," J. Mater., 2014, doi: https://doi.org/10.1155/2014/138163.

[54] T. Trupti, C. Abhishek, B. Rahul and D. Lokhande, "Lanthanum sulfide/graphene oxide composite thin films and their supercapacitor application," SN Appl. Sci., 2019, doi: https://doi.org/10.1007/s42452-018-0107-7.

[55] D. Sartale and C. Lokhande, "Growth of copper sulphide thin films by successive ionic layer adsorption and reaction (SILAR) method," Mater. Chem. Phys., 2000, vol. 65, pp. 63-67.

[56] Y. Obed, A. Dalia and M. Zeuz, "Deposition of Highly Crystalline Covellite Copper Sulphide Thin Films by SILAR," Phys. Status Solidi A Appl. Mater. Sci., 2017, doi: https://doi.org/10.1002/pssa.201700500.

[57] L. Seppo, A. Arnold and L. Markku, "Growth of CuS thin films by the successive ionic layer adsorption and reaction method," Appl. Surf. Sci., 2000, vol. 158, pp. 75-80.

[58] P. Mani, A. Janaki, A. Seelan and J. Prince, "Influence of Molar Concentrations on Optical Properties of Copper Sulphide Thin Films by Silar Method," Int. J. ChemTech Res., 2014, vol. 214, pp. 3573-3578.

[59] N. Ravindra, Y. Lee, J. Shm and C. Roh, "Chemical synthesis of 3D copper sulfide with different morphologies for high performance supercapacitors application," RSC Adv., 2016, vol. 6, pp. 14844-14851.

[60] M. Haneefa, M. Gani, S. Fareed and J. Raja, "The studies on optical and structural properties of zinc sulfide thin films deposited by SILAR method," J. Chem. Pharm. Res., 2015, vol. 7, pp. 141-145.

[61] M. Mana, K. Pankaj and M. Habib, "Fabrication and Characterization of ZnS based Photoelectrochemical Solar Cell," ES Energy Environ., 2020, vol. 12, pp. 77-85.

[62] V. Geetha and V. Rajan, "Studies of Structural and Optical Properties of Zinc Sulphide Thin Films," Int. J. Mater. Phys., 2014, vol. 5, pp. 5-14.

[63] S. Roy and P. Mitra, "Preparation of ZnS thin film by Silar," Mater. Sci. Res. India, 2008, vol. 5, pp. 447-452.

[64] G. Laukaitis, S. Lindroos and M. Leskela, "Stress and surface studies of SILAR grown ZnS thin films on(100)GaAs substrates," Mater. Sci. Eng. A., 2000, vol. 288, pp. 223-230.

[65] S. Lindroos, C. Bonnin and A. Leskea, "Growth and Characterization of Zinc Sulfide Thin Films Deposited by the Successive Ionic Layer Adsorption and Reaction (Silar) Method Using Complexed Zinc Ions As the Cation Precursor," Mater. Res. Bull., 1998, vol. 33, pp. 453-459.

[66] G. Hao, H. Shen and G. Chao, "The influence of annealing atmosphere on the phase formation of Cu–Sn–S ternary compound by SILAR method," J. Mater. Sci. Mater. Electron., 2013, vol. 24, pp. 3195–3198.

[67] D. Harshad, A. Lokhande, V. Raut and M. Patil, "Facile synthesis of Cu2SnS3 thin films grown by SILAR method: effect of film thickness," J. Mater. Sci. Mater. Electron., 2017, vol. 28, pp. 7912-7921.

[68] A. Aykut, "Structural and optical properties of Cu2SnS3 thin films obtained by SILAR method," Sakarya Univ. J. Sci., 2017, vol. 21, pp. 505-510.

[69] H. Shelke, A. Patil and C. Lokhande, "Electrochemical impedance analysis of SILAR deposited Cu2SnS3 (CTS) thin film," Int. J. Eng. Res. Technol., 2017, vol. 10, pp. 578-586.

[70] S. Mane, D. Lokhande and B. Sankapal, "Successive ionic layer adsorption and reaction (SILAR) method for the deposition of large area (~10 cm2) tin disulfide (SnS2) thin films," Mater. Res. Bull., 2000, vol. 35, pp. 2027-2035.

[71] P. Mani, K. Manikandan and J. Prince, "Influence of molar concentration on triethanolamine (TEA) added tin sulfide (SnS) thin films by SILAR method," J. Mater. Sci. Mater. Electron., 2016, vol. 27, pp. 9255-9264.

[72] P. Mitra and A. Mukherjee, "Structural and optical characteristics of SnS thin film prepared by SILAR," Mater. Sci. Poland, 2015, vol. 33, pp. 847-851.

[73] G. Biswajit, M. Das, B. Pushan and S. Das, "Fabrication and optical properties of SnS thin films by SILAR method," Appl. Surf. Sci., 2008, vol. 254, pp. 6436-6440.

[74] Y. Qachaou, O. Daoudi, A. Raidou and M. Fahoume, "The influence of solution temperature of SnS thin films grown by successive ionic layer adsorption and reaction (SILAR) method," IOP Conf. Ser. J. Phys., 2019, doi: https://doi.org/10.1088/1742-6596/1292/1/012022.

[75] B. Asta, B. Ieva and P. Anton, "The impact of thermal treatment on the structural, optical and electrochemical characteristics of tin sulfide films," Coatings, 2024, doi: https://doi.org/10.3390/coatings14101284.

[76] K. Ambily, K. Ali, V. Geetha and P. Kannan, "Towards phase pure CZTS thin films by SILAR method with augmented Zn adsorption for photovoltaic application," Mater. Renew. Sustain. Energy, 2019, doi: https://doi.org/10.1007/s40243-019-0152-1.

[77] G. Kumar, P. Balaji, P. Gnana and R. Kaushik, Investigations on SILAR coated CZTS thin films for solar cells applications," Phase Transit., 2021, https://doi.org/10.1080/01411594.2021.1939874.

[78] B. Gayatri, S. Das and S. Ghosh, "Optical Properties of Cu2ZnSnS4 (CZTS) Made By SILAR Method," Mater. Today Proc., 2019, vol. 18, pp. 494-500.

[79] M. Sawanta, P. Patil, W. Oh and A. Betty, "Synthesis and characterization of Cu2ZnSnS4 thin films by SILAR method," J. Phys. Chem. Solids, 2012, vol. 3, pp. 735-740.

[80] A. Vijendra, S. Dargad, A. Rajesh and K. Govind, "Fabrication of Highly Conducting Ag2S Thin Films on FTO Substrate by Using SILAR," Adv. Mater. Res., 2022, https://doi.org/10.4028/p-9k8hwu.

[81] C. Lokhande, B. Sankapal and R. Mane, "A new chemical method for the preparation of Ag2S thin films," Mater. Chem. Phys., 2000, vol. 63, pp. 226-229.

[82] B. Kakade, P. Nikam and R. Gosavi, "Effect of immersion cycles on structural, morphology and optoelectronic properties of nanocrystalline Ag2S thin films deposited by SILAR technique," IOSR J. Appl. Phys., 2014, vol. 6, pp. 6-12.

[83] R. Gosavi, S. Patel, R. Patil and M. Jadhav, "Studies on Characterization of Nanocrystalline Silver Sulphide Thin Films Deposited by Chemical Bath Deposition (CBD) and Successive Ionic Layer Adsorption and Reaction (SILAR) method," Arch. Phys. Res., 2011, vol. 2, pp. 27-35.

[84] S. Sadovnikov, A. Gusev and A. Rempel, "Nanocrystalline silver sulfide Ag2S," Rev. Adv. Mater. Sci., 2015, vol. 41, pp. 7-19.

[85] H. Shen, X. Jiao, D. Oron and H. Lin, "Efficient electron injection in non-toxic silver sulfide (Ag2S) sensitized solar cells," J. Power Sources, 2013, vol. 240, pp. 8-13.

[86] M. Deshpande, C. Krisha, P. Kiran and P. Rajput, “Study of Sb2S3 thin films deposited by SILAR method,” Mater. Res. Express, 2018, doi: https://doi.org/10.1088/2053-1591/aac4ef.

[87] Sankapal, R.; Mane, R.; Lokhande, D. Preparation and characterization of Sb2S3 thin films using a successive ionic layer adsorption and reaction (SILAR) method. J. Mater. Sci. Lett. 1999, 18, 1453-1455.

[88] Yang, Q.; Chen, Q.; Gong, F. Fabrication of MnCoS Thin Films Deposited by the SILAR Method with the Assistance of Surfactants and Supercapacitor Properties. Coatings. 2023, doi: https://doi.org/10.3390/coatings13050908.

[89] Garcia, V.; Collado, A.; Leal, D., Gonzalez, D. Synthesis and characterization of antimony sulfide thin films obtained by pulsed laser assisted chemical bath deposition. Mater. Chem. Phys. 2025, doi: https://doi.org/10.1016/j.matchemphys.2025.131081.

[90] Yue, Z.; Zhang, Z.; Hao, Z.; Wang, J. Electrodeposition of diamond-like carbon films on micro-textured surfaces. Diam. Relat. Mater. 2025, doi: https://doi.org/10.1016/j.diamond.2025.112649.

[91] Bo, F.; Yang, Y.; Jiong, D.; Gao,C. Co-sputtered thin films of silver-ion-conductive GeS2-Sb2S3-AgI solid electrolytes. Thin Solid Films. 2025, doi: https://doi.org/10.1016/j.tsf.2025.140769.

[92] Gao, X.; Li, Z.; Sun, R.; Lin, Z. Emerging materials and applications from thermally evaporated electronic films,” Mater. Sci. Eng. R. Rep. 2025, doi: https://doi.org/10.1016/j.mser.2025.101077.

[93] Deepa, S.; Salim, A.; Jassi, J. Spray-Pyrolysed Tin doped Zinc Oxide Thin Films-Analysis Based on Microstructural, Optical and Morphological Characterisations. Results Surf. Interfaces, 2025, doi: https://doi.org/10.1016/j.rsurfi.2025.100624.